Annals of R.S.C.B., ISSN:1583-6258, Vol. 25, Issue 6, 2021, Pages. 10697 - 10718
Received 25 April 2021; Accepted 08 May 2021.

Compare the Color Digital Image with JPEG 2000 and JPEG with Re-Size by Developing new Algorithm

Haeder Talib Mahde Alahmar
Al-Furat Al-Awsat Technical University, Iraq
haider.alahmer@atu.edu.iq
ORCID ID: http://orcid.org/0000-0002-5213-2393

ABSTRACT

Image compression is important over time, controls communication channels, and the great need for real-time data transfer. On this basis, many compression algorithms reduce the size of data on the condition that quality is maintained to the extent possible. In this research, we have a special interest in processing the objects that appear when processing digital images (specific space) given by the number of colors, such as those found in color coding (HSL or Green Blue Red (RGB)). A sophisticated algorithm has been created by relying on the intermittent interlock of image windows and computation of its assembly funcEnergy-Efficienttions using the process of centralization in all its different forms such as computation of arithmetic mean, geometric mean or arithmetic mean, all to be reduced and reconstructed for this colored digital space image. In this paper, we also present procedures for calculating the distortion resulting from reduction and reconstruction to evaluate the status of using the assemblages.

Keyword's
interpolation distortion, image compression, waveform conversion, JPEG2000, Wavelet, DCT, RGB, JPEG

Introduction

Communication is one of the most advanced areas of research, especially with a variety of tools of communication, the images are one of the most widely distributed types of data transmitted on the network, which is a motivation for research in black and white image compression algorithms and then color images that follow a standard color-coding system and multi-codec and multi-spectral imaging studies. Several research papers have been published on the subject of improving the quality of the compressed multi-spectral image, some of which mainly improve the image using a technique based on a very high-resolution technique [1]to estimate the high-resolution image of a low-resolution image.

Compression Component Analysis (PCA)

provides good comprehensive pressure for spectral saturated images, but the loading of basic compounds may fail in collecting discriminate information for saturated images. Since these are very important for classification functions, its energy may be weak within the energy of the quantitative signal. To address this problem, the researchers suggested in [2]a pressure method for spectral saturated spectra with a pre-coding process for discriminating polymorphic.

Some methods

have been introduced to improve the quality of satellite images, including a method that relies on both experimental transform and morphological filtration [3].

The proposed algorithm

Annals of R.S.C.B., ISSN:1583-6258, Vol. 25, Issue 6, 2021, Pages. 10697 - 10718
Received 25 April 2021; Accepted 08 May 2021.

Compresses performance improvement by relying on assembly functions by:

- Reduction using the three methods of aggregation, the arithmetic mean, the geometrical mean and the arithmetic mean, and using various color and space images their dimensions are different.
- Study the impact of the dimensions of the mass taken from the image where implementing the previous assembly, and calculate the value of the error resulting from the reduction and reconstruction of each block and frequency the process increases with cluster size.
- Study the impact of noise accompanying the performance of the reduction in the removal or mitigation of noise in the digital image by performing reduction and then the reconstruction.

Color Spaces

Rgb Color Space

The RGB color model is a group chromatic model, where red, green, and blue are grouped together and in different ways to form a matrix of colors. The primary objective of the RGB color model is to display the image and represent it with electronic systems such as television and computers. The three main colors (red, green, and blue) are mixed with different intensities of each vehicle to shape the desired color. If the optical intensity is not present for all vehicles, it gives black color., This leads to the formation of the white color [4].

Color Space YCbCr:

Is a secondary space that produces the basic colors in the RGB model by mixing two colors of the others (red, green, and blue) to produce our colors blue-green, red-violet, yellow, and adding color four to this space which is a black color to become CMYK space and uses this space to print on the carton.

Color space

YCbCr the YCbCr color space is used for video imaging and digital systems. Vehicle Y represents the brightness, and vehicle Cb represents the blue minus the brightness (B-Y) and Cr is the red color, which is also less bright [4].

Color System HSB, HSV

Hue, Saturation, Value (HSV) is a linear transformation from the basic color scheme, developed for Photoshop's famous photo editing software.

Color model

Hue, Lightness, Saturation (HLS) as HSV predecessor, is a linear transform model of the system RGB [4].

Annals of R.S.C.B., ISSN:1583-6258, Vol. 25, Issue 6, 2021, Pages. 10697 - 10718
Received 25 April 2021; Accepted 08 May 2021.

Color System YIQ

This system is used in television broadcasters, where the Y-ray and I-Q are chromaticity or in-phase quadrature [5].
The transform from RGB to YIQ is:

$$\begin{bmatrix} Y \\ I \\ Q \end{bmatrix} = \begin{bmatrix} .299 & .587 & .114 \\ .701 & -.587 & -.114 \\ -.299 & -.587 & .886 \end{bmatrix} \begin{bmatrix} R \\ G \\ B \end{bmatrix} \dots\dots\dots (1)$$

The transform from YIQ to RGB is:

$$\begin{bmatrix} R \\ G \\ B \end{bmatrix} = \begin{bmatrix} 1.000 & 1.000 & .000 \\ 1.000 & -.509 & -.194 \\ 1.000 & .000 & 1.000 \end{bmatrix} \begin{bmatrix} Y \\ I \\ Q \end{bmatrix} \dots\dots\dots (2)$$

COMPRESSION ALGORITHMS

Compression is organizing information using the least number of bits or units carrying information from an unencrypted representation. The compression helps reduce resource consumption such as hard disk space or transmission bandwidth. We will present a summary of the most important algorithms performed: JPEG and JPEG 2000.

Compression algorithm

Image compression is performed using the multiplexing JPEG technique in Figure. 1, where it is first converted to Discrete Cosine Transformation (DCT), which represents data and data as a packet of high and low frequencies. High frequencies indicate areas of fine and high detail. Low frequencies indicate the general view of the low-detail image.

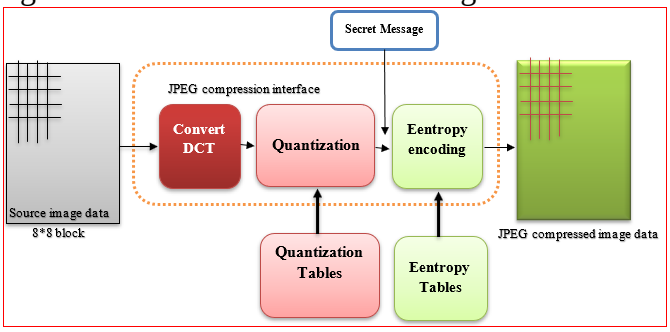

Figure.1 Image compression stages using JPEG

It is possible to delete fine details so the human eye is less sensitive in those areas. To illustrate this idea, we imagine a dense dark forest. If we randomly change a random set of pixels to black, the probability of seeing these pixels is very small and almost non-existent, because the human eye will be distracted by other details, whereas if this picture or painting Painted on a wall that is fully plated, we can easily see these black pixels (except for the black-painted wall of course) [5].

The algorithm can be summarized as follows

- The convert's pixels from the basic RGB format to YCbCr the color image combines three red, green, and blue (RGB) images, each representing a grayscale image. Each pixel of the color image carries different values of the three compounds to form the desired color. The JPEG algorithm starts with the transform from the RGB color system to the YCbCr system.

Annals of R.S.C.B., ISSN:1583-6258, Vol. 25, Issue 6, 2021, Pages. 10697 - 10718
Received 25 April 2021; Accepted 08 May 2021.

Y Vehicle (as we mentioned earlier) is the optical light vehicle, a linear installation of the three basic colors, the two vehicles represent the difference between the luminaries and each the red-blue alone, and common knowledge eye observation of the compound the first axis starts from blue and ends in yellow, the other axis starts from the red color and ends in yellow. Figure. 2 shows how to convert it. It is carried out according to these equations:

$$\begin{pmatrix} Y \\ Cb \\ Cr \end{pmatrix} = \begin{pmatrix} 0.2126 & 0.7152 & 0.0722 \\ -0.1146 & -0.3854 & 0.5 \\ 0.5 & -0.4542 & 0.0458 \end{pmatrix} * \begin{pmatrix} R \\ G \\ B \end{pmatrix} \dots\dots\dots\dots\dots (3)$$

$$\begin{pmatrix} R \\ G \\ B \end{pmatrix} = \begin{pmatrix} 1 & 0 & 1.402 \\ 1 & -0.34414 & 0.71414 \\ 1 & 1.772 & 0 \end{pmatrix} * \begin{pmatrix} Y \\ Cb - 128 \\ Cr - 128 \end{pmatrix} \dots\dots\dots\dots (4)$$

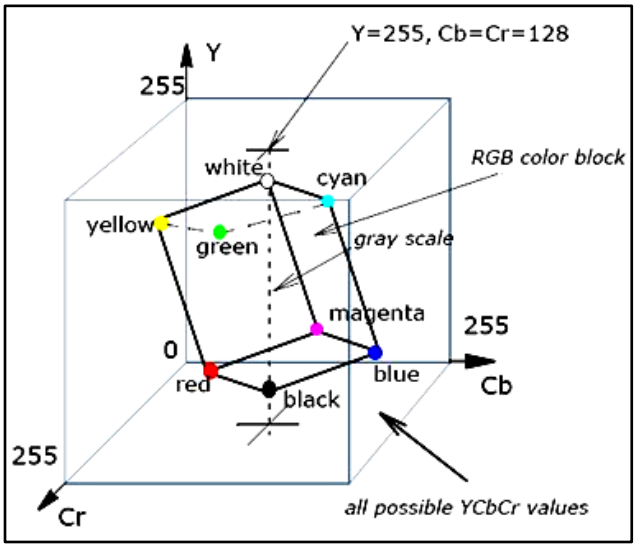

Figure2spatial representation of the YCbCr color model [6]

- Reduction of the representation of color compounds Subsampling:

At this stage, the representation of the chromatic compounds is reduced orreduced information about these compounds without reducing the quality of the image. The eye observes changes in the optical compounds rather than color compounds. There are several models of the reduction process in Figure . 3 where we have the basic model 4: 4: 4. Each vehicle has Y, Cr, and Cb and Model 2: 2: 4. Each vehicle has one vehicle of Cb and one of Cr. Because the eye will not notice the droplets that occur on the color compounds, therefore, this procedure will not affect the quality of the image.

Annals of R.S.C.B., ISSN:1583-6258, Vol. 25, Issue 6, 2021, Pages. 10697 - 10718
Received 25 April 2021; Accepted 08 May 2021.

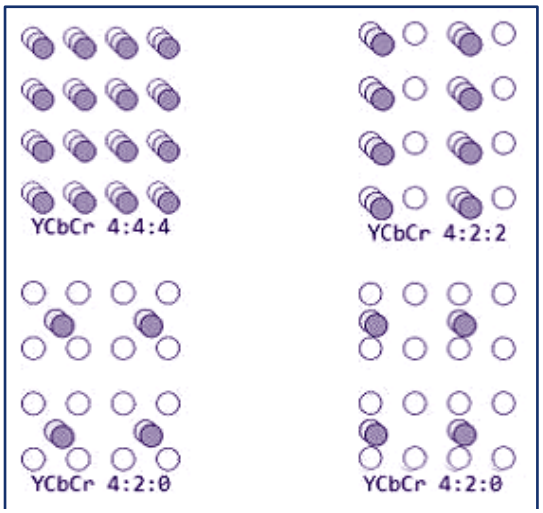

Figure3 Models of reducing the representation of chromatography YCbCr

Converts values to the bandwidth by using two-dimensional intermittent transponder transform: DCT[7] blocks 8 x 8 pixels of the image and converts them to 64 the following mathematical relationship frequency describes the mechanism of calculating DCT 2D constants:

$$G_{u,v} = \sum_{x=0}^{\cdot/} \sum_{y=0}^{\cdot/} a\,(u)a(v)g_{x.y}cos\left[\frac{\pi}{8}\left(x+\frac{1}{2}\right)u\right]cos\left[\frac{\pi}{8}\left(y+\frac{1}{2}\right)v\right] \ldots\ldots\ldots (5)$$

$$a(u) = \begin{cases} \sqrt{\frac{1}{8}}\, tfu = 0 \\ \sqrt{\frac{2}{8}}\quad O.W \end{cases} \quad \ldots\ldots\ldots\ldots\ldots\ldots\ldots\ldots\ldots (6)$$

The values of the transient's u, v vary between (0.8) and the number of lines and columns in each block. Gx. y represents the pixel value at the line and the column GU, v, y represents the intermittent query constantly. (4) The parameter in the upper left corner of the resulting mass is the coefficient of the highest value among the other constants. This constant is called the DC constant. This is the average of the pixel values within the mass. The rest of the constants, which number are non-continuous transactions AC. The obvious power in using this DCT is to assemble the lower frequencies in the upper corner of each block, which makes it easier to work in the next stages, but we may have a problem here: that the intermittent transform of the input causes the depth of the bits to increase, the values of the pixels, but after applying the intermittent transformations to them, may show us values that need 16 bits to be represented. Hence the importance of quantization, which is the next stage after the transform of the intermittent query. At this stage, we re-represent the pixel values on eight bits [8].

To return to the basic values (pixel values) we had, we can apply the following intermittent IDCT test described in the following relationship:

$$\boldsymbol{f(x,y) = \sum_{u=0}^{7} \sum_{v=0}^{7} F\,(u,v) \frac{Cu}{2} \frac{Cv}{2} cos\left[\frac{(2x+1)u\pi}{16}\right] cos\left[\frac{(2y+1)v\pi}{16}\right]} \ldots (7)$$

- Quantization:

The phase of quantification comes as a continuation of the previous phase to reduce the information that represents the high-frequency vehicles that the human eye cannot distinguish [7].

Annals of R.S.C.B., ISSN:1583-6258, Vol. 25, Issue 6, 2021, Pages. 10697 - 10718
Received 25 April 2021; Accepted 08 May 2021.

This is done by dividing the transactions resulting from a transforming phase using a quantization Table whose laboratory values vary according to the quality required after the compression process. (4) Is a numerical example of the process of frequency transform and quantification: (1)

Table 1.DCT and quantization (numerical example)

139	144	149	153	155	155	155	155	235.6	-1.0	-12.1	-5.2	2.1	-1.7	-2.7	1.3	16	11	10	16	24	40	51	61
144	151	153	156	159	156	156	156	-22.6	-17.5	-6.2	-3.2	-2.9	-0.1	0.4	-1.2	12	12	14	19	26	58	60	55
150	155	160	163	158	156	156	156	-10.9	-9.3	-1.6	1.5	0.2	-0.9	-0.6	-0.1	14	13	16	24	40	57	69	56
159	161	162	160	160	159	159	159	-7.1	-1.9	0.2	1.5	0.9	-0.1	0.0	0.3	14	17	22	29	51	87	80	62
159	160	161	162	162	155	155	155	-0.6	-0.8	1.5	1.6	-0.1	-0.7	0.6	1.3	18	22	37	56	68	109	103	77
161	161	161	161	160	157	157	157	1.8	-0.2	1.6	-0.3	-0.8	1.5	1.0	-1.0	24	35	55	64	81	104	113	92
162	162	161	163	162	157	157	157	-1.3	-0.4	-0.3	-1.5	-0.5	1.7	1.1	-0.8	49	64	78	87	103	121	120	101
162	162	161	161	163	158	158	158	-2.6	1.6	-3.8	-1.8	1.9	1.2	-0.6	-0.4	72	92	95	98	112	100	103	99
Basic image sample								constant value DCT								Quantization table							
15	0	-1	0	0	0	0	0	240	0	-10	0	0	0	0	0	144	146	149	152	154	156	156	156
-2	-1	0	0	0	0	0	0	-24	-12	0	0	0	0	0	0	148	150	152	154	156	156	156	156
-1	-1	0	0	0	0	0	0	-14	-13	0	0	0	0	0	0	155	156	157	158	158	157	156	155
0	0	0	0	0	0	0	0	0	0	0	0	0	0	0	0	160	161	161	162	161	159	157	155
0	0	0	0	0	0	0	0	0	0	0	0	0	0	0	0	163	163	164	163	162	160	158	156
0	0	0	0	0	0	0	0	0	0	0	0	0	0	0	0	163	164	164	164	162	160	158	157
0	0	0	0	0	0	0	0	0	0	0	0	0	0	0	0	160	161	162	162	162	161	159	158
0	0	0	0	0	0	0	0	0	0	0	0	0	0	0	0	158	159	161	161	162	161	159	158
Constant value DCT								Reverse quantization of Constants								Recovered image samples (IDCT0)							

- Encoding Run-Length RLC Coding on AC Transactions:

Typical model DCTs are often full of zeros, and we find that only a few values have numbers other than zero, and we can implicitly assume that nonzero numbers are present in the upper left-hand side of the transactions (low-frequency compounds), and zeros are restricted in the lower right-hand side (high-frequency vehicles), so the resulting transactions are rearranged using the Zag Zig method in Figure . (5) so, zero values are ignored and the value of the next zero is ignored [9].

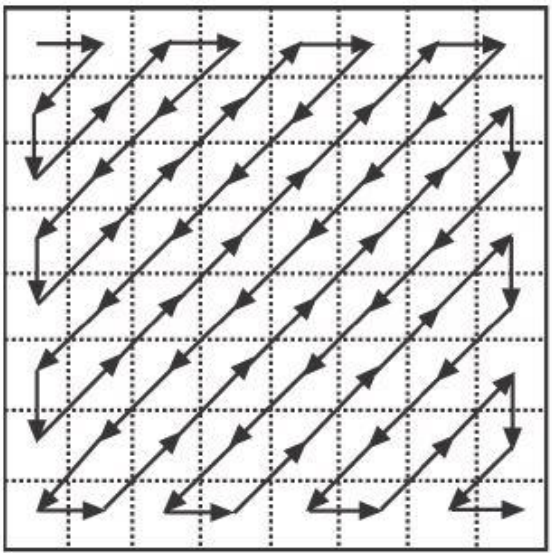

Figure4 Mechanism of aggregation of DCT coefficients by Zag Zig method[10]

- Differential Pulse Code Modulation DPCM:

DC continuous transactions are coded separately from non-continuous transactions, using DPCM, if the constant transaction values for the first five blocks are:

Annals of R.S.C.B., ISSN:1583-6258, Vol. 25, Issue 6, 2021, Pages. 10697 - 10718
Received 25 April 2021; Accepted 08 May 2021.

144, 152, 149, 155, 150 shall have a cryptographic output - 8, 3, - 6, 5, 150 = di so that = di DCi + 1 - DCi and primary value[11].

- Intuitive coding:

The last stage of the image compression process is the intonation coding, and this phase is an additional step to get more compression of the data so that the coding for both continuous and non-continuous transactions is returned to the previous example when we get - 8, 3, 6, 5, 150 = The coding process is:
Each parameter is represented in the form (size, width) so that the size is expressed as the number of bits required to encode the parameter while the argument represents the parameter value, thus representing values:
(1011, 3) (101, 3) (10010110, 8) The size is finally encoded using Hoffman's encoding, but the encoder is not encoded because its value varies widely and Hofmann's encoding will not be useful [3].

Compression algorithm JPEG 2000

A new standard in image and video compression extends the JPEG standard. Many advanced imaging camerashave supported this compression technology. This compression technology supports several levels of accuracy or quality and has a higher compression accuracy than JPEG. 20% compression higher than JPEG compression technology. The basic difference in the working mechanism between JPEG and 2000 JPEG is the first adoption of the transform and the last adoption of the wave transform [12].
Figure. (6) shows the box diagram of pressure and pressure decompression according to the JPEG2000 technique

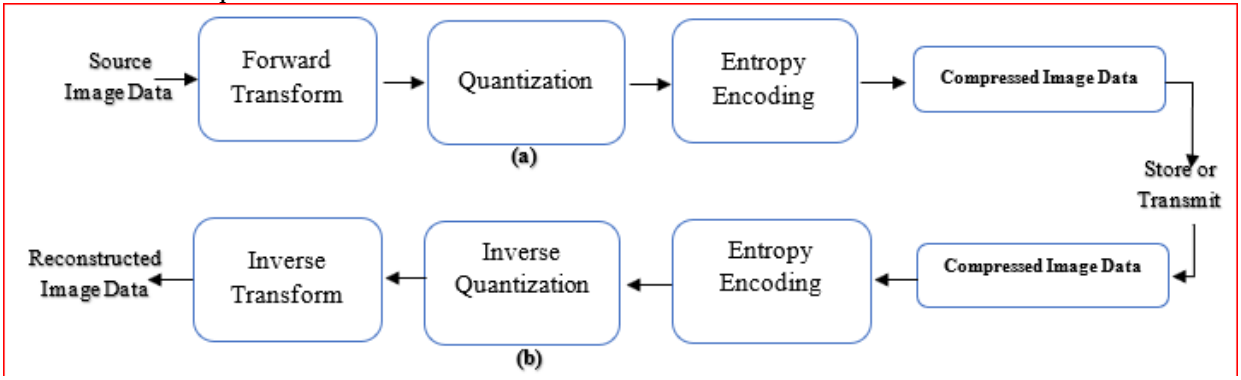

Figure5 Pressure and decompression according to JPEG2000 technique
The main difference between JPEG and JPEG 2000 is the transform coefficients.
The steps followed by the JPEG 2000 standard are [13]:

- Reinstalling the original image with new vehicles or components.
- Reconstructing the new image elements with rectangular tiles, which are the primary component of the original image reconstruction.
- Apply the wavelet on each tile independently and through the tile is re-installed at different levels of accuracy.

Annals of R.S.C.B., ISSN:1583-6258, Vol. 25, Issue 6, 2021, Pages. 10697 - 10718
Received 25 April 2021; Accepted 08 May 2021.

Image compression and re-installation using the Discrete Rajan Transform based on spectral dispersion

The previously intermittent Rajan transform was used in the propagation and compression of speech data in the spectral domain, where it was applied to sound data, and the result was propagated by maintaining the Cumulative Point Index CPI (i.e. the cumulative point index) and forcing other spectral compounds to be zero. Later, the intermittent Rajan transform (DRT) was used to compress and scatter the images.

- Operation Sparsafication in Rajan Transform:

The Rajan transform (RT) is the alternative to the Hadamard Transform, which was developed primarily for pattern recognition, and Rajan's transform has a homomorphic and fixed-variant nature, [14]and this property of the Rajan transform It has many applications in edge detection algorithms, ocean detection and detection of curves and lines in images and isolating some points in them. With the help of an algorithm, prose representation can be obtained without loss or loss [9].

The process of prose is defined as the process by which most coefficients and coefficients are made zero or close to zero, where a beam far away from N is said to be a signal if most of its coefficients are zero or close to zero. If there is a non-zero k coefficient, and the rest of the N-K workers are zero, then we say it is a signal with a K coefficient. The power distribution determines sparsity of the signal. If the energy distribution is a super energy value represented by one parameter and all remaining zero transactions, Prosthetic, this signal is highly compressible. The proportional degree to indicate defined as the ratio of the number of zero or near zero samples to the full number of samples representing the signal [15]:

Sparsity = ((N-K)/N) *100

Where N-K represents the number of zero values and near-zero, N represents the total of transactions, K represents the number of non-zero transactions.

Prose determines the number of non-zero transactions in which the entire signal energy is distributed. The higher prose, the greater the number of non-zero coefficients distributed among them. The higher prose, the greater the number of zero coefficients and near zero. More information on prose can be obtained in Rajan's transform in Ref [16].

- The pressure can be summed up using the Rajan transform:

Figure . (7) shows the box diagram of the image compression process using Rajan transform. The process can be summarized:

a. Insert a picture with W * W dimensions.
b. Convert the image to a line of length W *W.
c. Clear the image with 8 length blocks each.
d. Apply the intermittent Rajan transform on the selected beam and obtain the spectral series for the intermittent Rajan transformation.
e. Store the value of the CPI and the value of the intermediate spectral vehicle in the derived spectral series, while the rest of the spectral parameters are forced to be zero.
f. Re-complete the procedure until the image is scanned and processed.
g. The resulting series is then scattered spectral series.
h. Apply the Run Length Encoding (RLE) algorithm and compute the compression rate.
i. Apply the decompression algorithm to obtain the spectral series.

Annals of R.S.C.B., ISSN:1583-6258, Vol. 25, Issue 6, 2021, Pages. 10697 - 10718
Received 25 April 2021; Accepted 08 May 2021.

j. Apply the intermittent RJAN Reverse Inverse DRT transform to reconstruct the image [9].

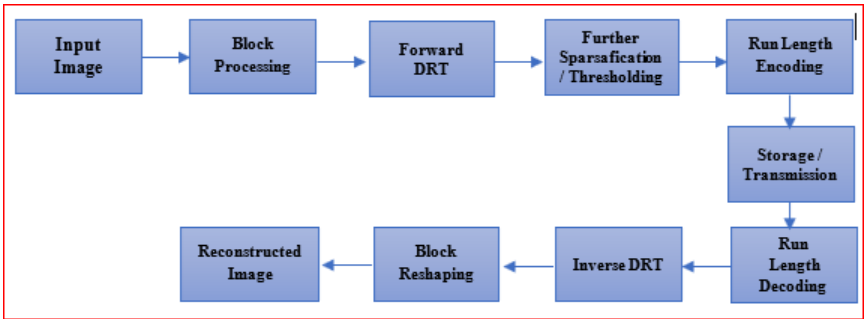

Figure6 Fund diagram of the image compression process using DRT transform

Proposed algorithm

It is an advanced algorithm for compressing and reconstructing digital color images based on its assembly functions using a differentiation process such as arithmetical calculation, geometric mean or arithmetic mean [17].

This algorithm determines which methods are better in terms of yield and deformation. To determine the effectiveness of the algorithm in the treatment of noise of various types added to the images carried out reduction and reconstruction because of the use of different assembly functions. Let Q be a digital image of size N X M. Here are the steps of the algorithm:The image is divided into non-intersecting fractional blocks of equal dimensions, and nXn is the mass dimensions. If M or N is not divisible by n, the lines and columns are removed to achieve division.

- Subsidiary the Centering (F).
- For each block in the Q image, do:

a. Calculate the value of the broker's median child.
b. Replace the block with the resulting value [18].

Figure . (8) shows an illustration of the MD5 algorithm.

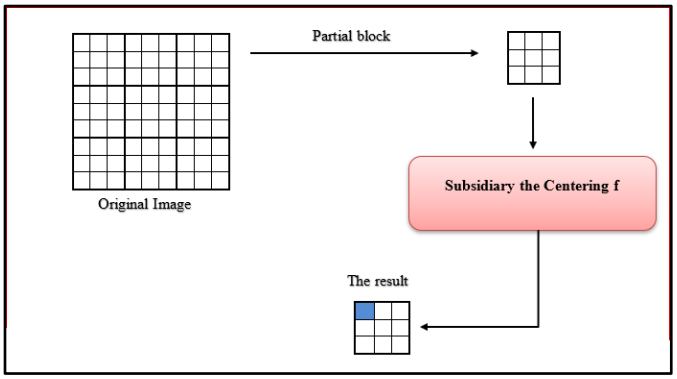

Figure7 an illustration of the reduction algorithm

The schematic diagram described in Figure. (9) summarizes the basic stages of algorithm work:

Annals of R.S.C.B., ISSN:1583-6258, Vol. 25, Issue 6, 2021, Pages. 10697 - 10718
Received 25 April 2021; Accepted 08 May 2021.

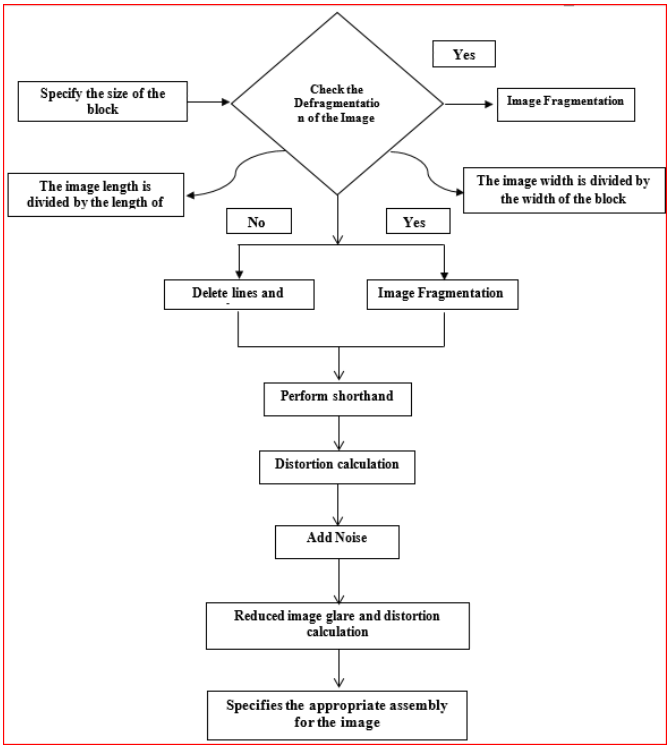

Figure8 the basic stages of algorithm work

Reconstruction

The reconstruction process is based on mathematical interpolation[19]where interpolation is meant to calculate the pixel values in the selected mass of the reduction and the size of the original image. The following is the general reconstruction algorithm using interpolation.
Where the process can be completed in several ways including:

- Nearest Neighbor Interpolation

This method is based on reading the values of each pixel in the reduced image and repeating it within the mass. This method does not add new values to the computed values, so it is easily and quickly executed, but the resulting image suffers from fracture [15].

- Bilinear interpolation

In this method of interpolation, the average values of adjacent pixels are calculated in the reduced image, and the calculated value in the cluster is repeated. This method is better than the previous method.

- Cubic Convolution Interpolation [20]. This method calculates the average of 16 adjacent pixels in the reduced image and repeats this value in the mass. This method is characterized by giving a clearer picture of the binary method.

The first method in this study was adopted in reconstruction, which is the closest neighbor method (because it is practical, easy to apply, and simple mathematical (which we chose due to

Annals of R.S.C.B., ISSN:1583-6258, Vol. 25, Issue 6, 2021, Pages. 10697 - 10718
Received 25 April 2021; Accepted 08 May 2021.

our limited technological limitations and computing capabilities) (but at the expense of precision [16]).
(The execution speed was chosen instead of precision) [21].
Figure. (10) illustrates an illustration of the decoding algorithm.

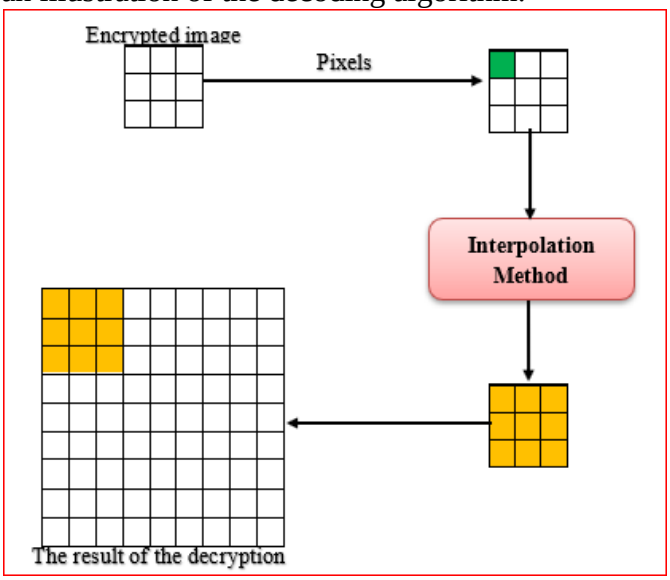

Figure9 an illustration of the decoding algorithm.

Practical Application

The Matlab 2017a simulation software was used to implement the algorithm and to show and calculate the results. It is a leading program in engineering and sports applications produced by MathWorks. This program allows mathematical manipulation of matrices, mathematical charting, implementation of various algorithms, creation of graphical user interfaces, and communication with programs written in other languages, including,C++, C, Java, and FORTRAN. Matlab is used with many other applications and utilities such as Simulink (Figure. 11) shows the MATLAB window and the sub-windows within it. Here are explanations [22]:

- Represents the editor, where here are written codes and algorithms.
- The place where the file will be saved represents the editor we have implemented and it is worth mentioning that the file is saved with the extension of m [23].
- The workspace represents where the values of the variables are displayed during the process of implementation of the program, and displays the final values of the transitions after the completion of the implementation (which helps us in the process of debugging) [21].
- The toolbar represents where we can through this tape to save the work file, play it, run simulation debugging, and a lot of other options.
- The details of the folder within the work file are displayed here.
- Error messages are displayed within this window called the command widow command (it is important to note that we can write commands directly and execute them in this window without having to write them in the editor) [24].

Annals of R.S.C.B., ISSN:1583-6258, Vol. 25, Issue 6, 2021, Pages. 10697 - 10718
Received 25 April 2021; Accepted 08 May 2021.

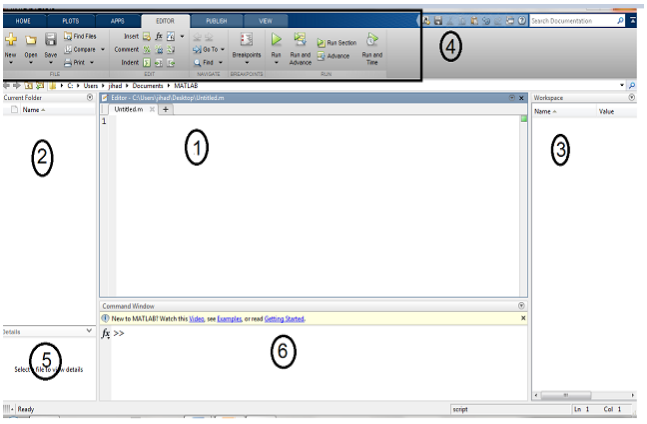

Figure 10.theMATLAB program main menu

The main menu of the program

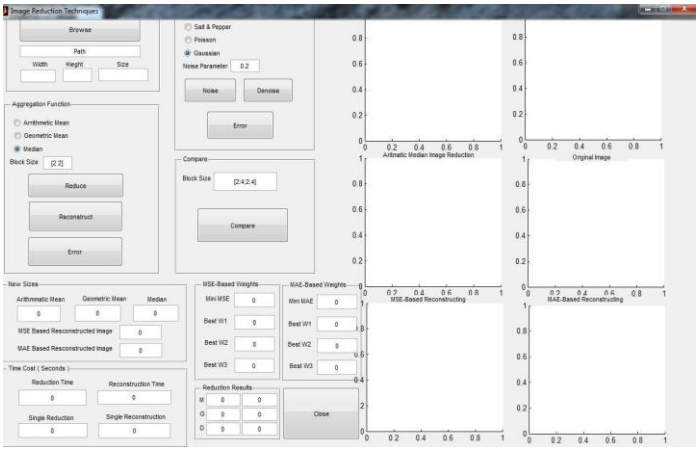

Figure 11. The main menu of the program

The main menu of the program, as shown in Figure . 12, allows ease of use by searching for the image, which takes the path of the file of this image and displays the image's determinants, size, average color, standard deviation, its proportion and its representation in the three methods mentioned above (arithmetic mean, the reduction yield (ie, the ratio of size after reduction to the previous one) has also been taken. It also enables the application of noise and the test of reducing performance in removing or reducing noise [25].

Implementation of Shorthand

The shorthand operation is performed by using one of the following assembly functions:

$$\boldsymbol{Mean} = \frac{\sum_{i=1}^{L} \boldsymbol{ni}}{\boldsymbol{L}} \quad \text{..... (8)}$$

Geometric Mean:

$$\boldsymbol{Mean} = \sqrt[L]{\boldsymbol{\Pi n_i}} \quad \text{..... (9)}$$

Arithmetic Median: Is an element of the group, half of which is smaller than half of the group elements, and half of it is larger. Thus, to find the center of a block, the elements of this cluster are ordered ascending or descending, and the item with the location is selected in the middle.

Annals of R.S.C.B., ISSN:1583-6258, Vol. 25, Issue 6, 2021, Pages. 10697 - 10718
Received 25 April 2021; Accepted 08 May 2021.

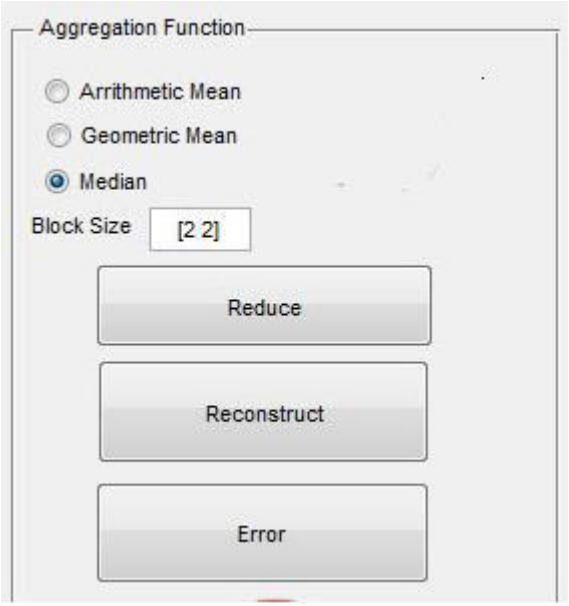

Figure12. Implementation of reduction and reconstruction

Calculation of deformation

n order to distort the image must be reconstructed from the reduced image, there are several ways to rebuild, we will rely on the simple method, which is to rebuild the cluster by repeating the pixel value of the size of the block and then calculate the deformation is calculated in two ways:

- The error in the quadratic mean and calculated by relationship:
  $\boldsymbol{MSE(Q, Q^1) = \frac{1}{NXM}\sum_N \sum_M (Q - Q^1)^2}$ **..... (10)**
- The error in absolute value is calculated by relationship:
  $\boldsymbol{MAE(Q, Q^1) = \frac{1}{NXM}\sum_N \sum_M |Q - Q^1|}$ **..... (11)**

Shorthand image sizes in three ways

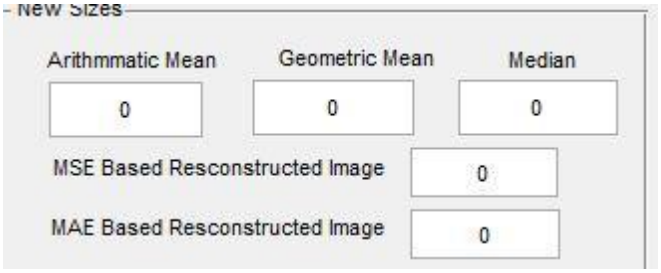

Figure13. the size of the image is reduced by the three methods

Add required noise

There are usually several types of noise in digital images, including:

- Salt and pepper: random pixels are selected in the image and a colored vehicle is also randomly selected and the value of the vehicle changes to either the lowest value or the highest possible value.

Annals of R.S.C.B., ISSN:1583-6258, Vol. 25, Issue 6, 2021, Pages. 10697 - 10718
Received 25 April 2021; Accepted 08 May 2021.

Poisson noise: artificial noise is generated and collected to the original image.

- Gaussian noise: Added white noise Guise collective of the digital image and gives the relationship:

$$\boldsymbol{PG(z)} = \frac{\mathbf{1}}{\sigma\sqrt{2\pi}} \boldsymbol{e}^{-\frac{(z-\mu)^{\mathbf{2}}}{2\sigma^2}} \quad \ldots\ldots\ldots\ldots\ldots (12)$$

Z = Mathematical gradients
μ = The value of the medium
σ = Standard Deviation

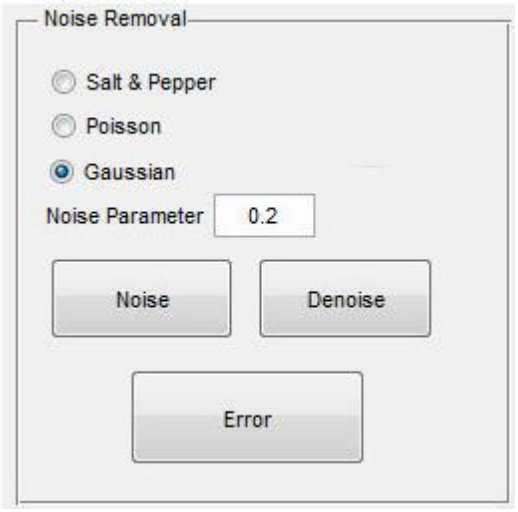

Figure 14. Add and remove noise

Executing shorthand on the glowing image and distortion calculation

The reduction function is tested to remove or reduce noise in the digital image by performing reduction and then the reconstruction.

The calculation cost of the reduction and reconstruction process

The time needed to reduce the image and time needed to restore the reduced image estimated in seconds:

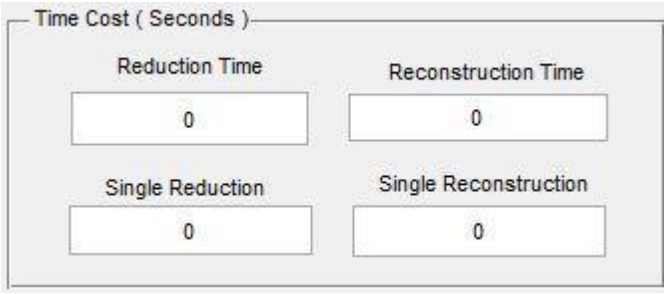

Figure15. the calculation cost of the reduction and reconstruction process

Choosing the best of the three methods of reduction in dependence on the smallest value of error is absolute error or square average error.

Annals of R.S.C.B., ISSN:1583-6258, Vol. 25, Issue 6, 2021, Pages. 10697 - 10718
Received 25 April 2021; Accepted 08 May 2021.

Figure16. optimal weight values

Study the impact of mass dimensions

The reduction was performed using the three methods of aggregation, namely the arithmetic average, the geometric mean, and the arithmetic mean of some different images in terms of structure and color-coding. Figure. (18) and Figure. (19) show the error curve in the square mean in terms of mass dimensions and the error curve in absolute terms in terms of mass dimensions change. Note that using the arithmetic mean of the reduction gives the best results as the mass dimensions increase.

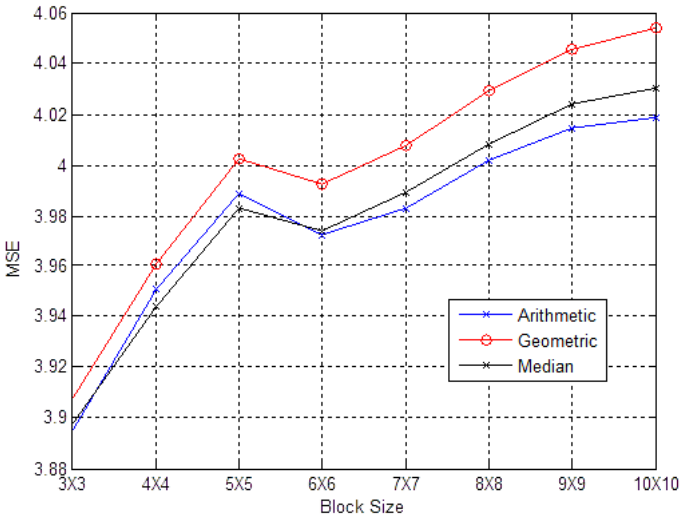

Figure17.the curve of the square mean in terms of mass dimensions

Annals of R.S.C.B., ISSN:1583-6258, Vol. 25, Issue 6, 2021, Pages. 10697 - 10718
Received 25 April 2021; Accepted 08 May 2021.

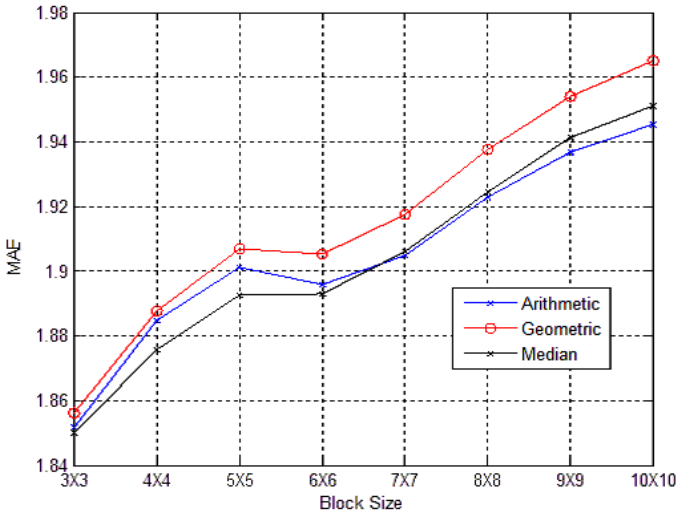

Figure18. gives the error curve in absolute value in terms of mass dimensions change

Comparison Results Between the Proposed Algorithm and Algorithm

The proposed algorithm was tested on many of the captured satellite images and was obtained as an electronic version of Damascus province later. And the size of these images
The first image is sized KB 11718The third image is 9635KB
The second image is sized KB 6591. The fourth image is KB 9365

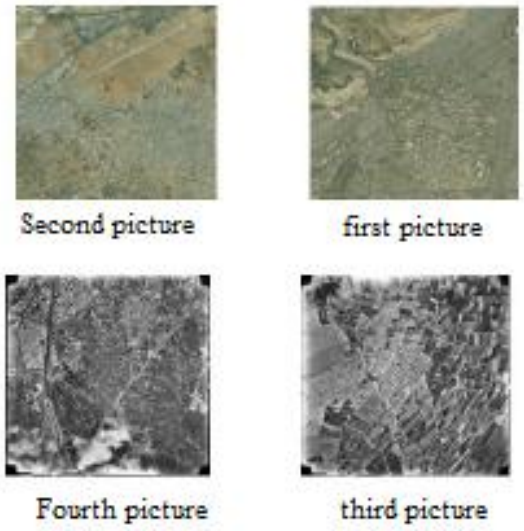

Figure19. Captured satellite images

After practical application, it was found that the image's strength before the pressure was 6591 KB and after the pressure became:

- **Using the 144KB method.**
- **Using the geometric mean method of 145KB.**
- **Using an arithmetical method of 157 KB.**

Annals of R.S.C.B., ISSN:1583-6258, Vol. 25, Issue 6, 2021, Pages. 10697 - 10718
Received 25 April 2021; Accepted 08 May 2021.

The pressure ratio was about 97% of the original size, approximately 126 seconds.
To ensure the algorithm is effective in reducing the noise in the digital images, this procedure was added so noise can be entered from different types on the images, for example, we added the noise of the drum by 0.2 coefficient and we implemented the program in terms of reduction and reconstruction, which reduces the noise was good results. Applying the proposed algorithm to the four images (using the three methods) and the comparison results in terms of the reduced image size between the proposed technology and the JPEG and JPEG 2000 technologies [26].

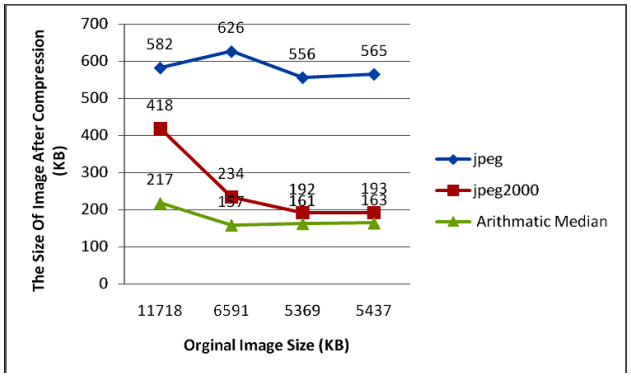

Figure20. Comparison of pressure performance using the arithmetic Median and technique JPEG and JPEG 2000

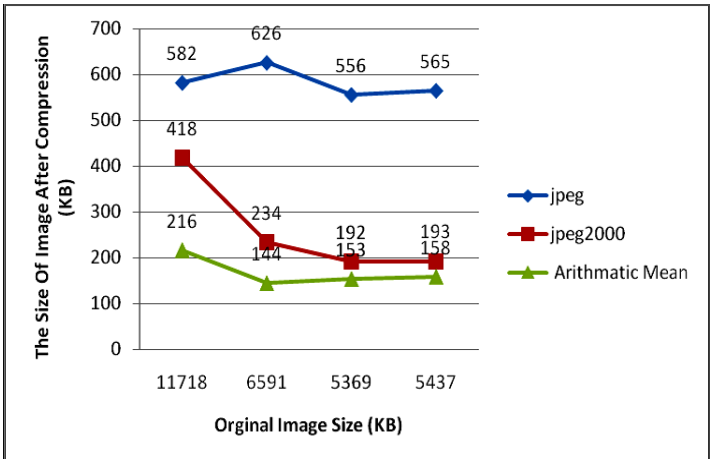

Figure21. Comparison of pressure performance using the arithmetic mean and technique JPEG and JPEG 2000

Note from previous formats that the compression ratio is not very different between the three methods but they differ greatly from.jpeg and 2000 jpeg. The difference between the three methods is evident by comparing coefficients in Table (2):

Table 2. SNR ،MAE between three methods

Arithmetic Mean	Arithmetic Mean	Arithmetic Median	Image size / Algorithm	Compare factor
30.7392	25.9835	17.20292	11718	MAE
20.435	18.998	12.3255	6591	
16.7684	15.49822	3.0492	5369	
5.462	10.3739	1.239	5437	
31.545	32.86409	59.6535	11718	SNR
18.8877	29.23287	48.3277	6591	
12.8548	18.03048	32.19118	5369	
13.532	14.19428	20.7765	5437	

.I

Annals of R.S.C.B., ISSN:1583-6258, Vol. 25, Issue 6, 2021, Pages. 10697 - 10718
Received 25 April 2021; Accepted 08 May 2021.

Conclusion

The study showed there is a clear difference between the pressure between the images resulting from the proposed algorithm and the images resulting from JPEG technology.

- For the third picture, the pressure ratio is 97% when using the proposed algorithm and 88% when using the JPEG algorithm.

The size of the images after compression using the proposed algorithm **(in the arithmetic mean) is less than the JPEG2000 compression image sizes. Despite the strength and wide use of this algorithm, the algorithm was obtained using the proposed algorithm:**

- For the first image, the pressure ratio using the proposed algorithm was 98.1% while JPEG2000 was 96.4%.

The reduction of the digital image using the arithmetic mean is the least distortion method followed by the geometric mean and then the arithmetic means when looking for the lowest error value MAE.

- The line increases as the mass dimensions increase. Increasing the dimensions of the mass increases the number of pixels whose values will change. Thus, the distortion will increase, although increasing the dimensions of the mass helps accelerate the reduction and reconstruction process.
- The reduction of noise using reduction using the arithmetic mean is the best method, where the mean is used to reduce the noise, especially the noise of the screw.

Acknowledgments

For all those who contributed to the success in ascending the level of algorithms and enable access to the real-time and thanks to the Iraqi University / Faculty of Engineering thanks to its software development environment**.**

SECNEREFER

[1] e. RADHAKRISHNA NAIK, "Periodic and Aperiodic Real -Time Task Scheduling Algorithms Simulator," International Journal of Pure and Applied Mathematics, pp. 2681-2687, 2017.

[2] H. L. J. L. J. K. P. &. K. B. B. Baek, "Real-Time Scheduling for Preventing Information Leakage with Preemption Overheads," Advances in Electrical and Computer Engineering, pp. 123-133, 2017.

[3] D. S. N. W. D. N. N. C. S. Lakew, "Aerial Energy Orchestration for Heterogeneous UAV-Assisted Wireless Communications," IEEE Systems Journal, vol. 1, no. 1, 2021.

[4] M. P. L. &. S. J. Schoeberl, "A multicore processor for time-critical applications,"

Annals of R.S.C.B., ISSN:1583-6258, Vol. 25, Issue 6, 2021, Pages. 10697 - 10718
Received 25 April 2021; Accepted 08 May 2021.

IEEE Design & Test, no. 2, pp. 38-47, 2018.

[5] B. a. H. K. Kada, "A fault-tolerant scheduling algorithm based on checkpointing and redundancy for distributed real-time systems," Research Anthology on Architectures, Frameworks, and Integration Strategies for Distributed and Cloud Computing, vol. Issue 7, 2021.

[6] J. a. A. S. Teraiya, "Optimized scheduling algorithm for soft Real-Time System using particle swarm optimization technique," Evolutionary Intelligence, no. No.20, pp. 1-11, 2021.

[7] C. Rochange, "Parallel real-time tasks, as viewed by WCET analysis and task scheduling approaches," in International conference proceedings, 2016.

[8] A. M. R. S. L. R. S. Fernanda F. Peronaglio, "Modeling real-time schedulers for use in simulations through a graphical interface," in In Proceedings of the 50th Annual Simulation Symposium, San Diego, CA, USA, 2017.

[9] D. T. M. ALAHMAR, "RANDOM TASK SCHEDULER ALGORITHMS AS A COMPARISON AND ACCESS TO THE BEST TO USE IN REAL TIME," International Journal of Scientific & Engineering Research, vol. 1, no. 5, pp. 529-522, April 2019.

[10] I. Tektronix, A Guide to MPEG Fundamentals and Protocol Analysis (Including DVB and ATSC), vol. 1, SW Karl Braun Drive, Beaverton: Tektronix, pp. 12-11.

[11] K. S. Lakshmanan, "Scheduling and Synchronization for Multi-core Real-time Systems," Carnegie Mellon University Pittsburgh, PA, 2019.

[12] Z. e. a. Chen, "Blocking analysis of suspension-based protocols for parallel real-time tasks under global fixed-priority scheduling," Journal of Systems Architecture, Jan 2021.

[13] M. e. a. Abdel-Basset, "EA-MSCA: An effective energy-aware multi-objective modified sine-cosine algorithm for real-time task scheduling in multiprocessor systems: Methods and analysis," Expert Systems with Applications, p. 173, 13 December 2021.

[14] G. F. S. S. C. P. I. &. B. S. Levin, "DP-FAIR: A simple model for understanding optimal multiprocessor scheduling," in In 2010 22nd Euromicro Conference on Real-Time Systems ., 2020.

[15] D. T. M. ALAHMAR, "SPEECH RECOGNITION BY IMPROVING THE PERFORMANCE OF ALGORITHMS USED IN DISCRIMINATION," International Journal of Computer Science & Information Technology, vol. 11, no. 1, pp. 29-19,

February 2019.

[16] R. K. GOKULSIDARTHTHIRUNAVUKKARASU*, "Scheduling Algorithm for Real-Time Embedded Control Systems Using Arduino Board," in KnE Engineering | The International Conference on Design and Technology, Australia, 2017.

[17] S. A. K. AMJAD MAHMOOD, "Energy-Aware Real-Time Task Scheduling in Multiprocessor Systems Using a Hybrid Genetic Algorithm," Electronics,, no. 2, 19 May 2017.

[18] K. M. Z. L. LINLINTANGA, "A New Scheduling Algorithm Based on Ant Colony Algorithm and Cloud Load Balancing," Harbin Institute of Technology Shenzhen Graduate School Shenzhen, China, 2016.

[19] R. M. J. M. J. C. B. N. &. T. D. Strong, "Fast Switching of Threads between Cores," ACM SIGOPS Operating Systems Review, pp. 35-45, 2009.

[20] S. X. M. L. C. P. L. T. G. C. S. O. &. L. I. Xi, "Real-time multi-core virtual machine scheduling in Xen," in 2014 International Conference on Embedded Software (EMSOFT), Jaypee Greens, India, 12-17 Oct. 2014.

[21] X. M. P. L. S. O. X. S. L. C. G. C. &. L. I., "Cache-aware compositional analysis of real-time multicore virtualization platforms," Real-Time Systems, p. pp 675–723, November 2015.

[22] V. SHINDE and S. C. BIDAY, "Comparison of Real Time Task Scheduling Algorithms," International Journal of Computer Applications, pp. 37-41, 2017.

[23] S. T. GIRISH, D. R. PRASHANT and R. DESHMUKH, "Performance Analysis of Real Time Task Scheduling Algorithm," International Journal of Innovative Research in Computer and Communication Engineering IJIRCCE, pp. 11866-11869, 2017.

[24] H. N. TRAN, "Cache Memory Aware Priority Assignment and Scheduling Simulation of Real-Time Embedded Systems," Brest.2017 ,.

[25] K. &. M. A. Anjaria, "Thread scheduling using ant colony optimization: An intelligent scheduling approach towards minimal information leakage," leakage. Karbala International Journal of Modern Science, pp. 241-258, 2017.

[26] M. A. e. a. El Sayed, "Energy-Efficient Task Partitioning for Real-Time Scheduling on Multi-Core Platforms," computers magazines, vol. 10, p. 10, 2021.

[27] K. R. R. a. P. C. Yip, Discrete cosine transform: algorithms, advantages, applications, Boca Raton: Taylor & Francis Group, 2019, p. 490.

[28] A. G. R. M. Gersho, Vector quantization and signal compression, Springer Science

Annals of R.S.C.B., ISSN:1583-6258, Vol. 25, Issue 6, 2021, Pages. 10697 - 10718
Received 25 April 2021; Accepted 08 May 2021.

&Business Media, p. 732 .

[29] N. .T, "Lossless Iterative Compression for HSI Using Combined LDA Feature and Channel Coding," International Journal of Advanced Research in Electrical,Electronics and Instrumentation Engineering, vol. 5, no. 5, pp. 4247-4240, May 2016.

[30] P. V. K. S. Gauri D. Rode, "Satellite Image Quality Improvement Using Wavelet Based Enhancement Method," International Journal of Advanced Research in Computer and Communication Engineering, vol. 5, no. 5, pp. 910-907, May 2016.

[31] N. PM, "VARIOUS COLOUR SPACES AND COLOUR SPACE CONVERSION," International Journal of Global Research in Computer Science, vol. 4, no. 1, pp. 44-48, 2013.

[32] K. P. M. V. S. Kethepalli Mallikarjuna, "Sparse representation based image compression using discrete Rajan transform," International Journal of Applied Engineering Research, pp. 33424-33429, August 2015.

[33] D. K. J. S. D. C. D. N. S. B. V. Bhagya Raju, "Multispectral image compression for various band images with high resolution improved DWT SPIHT," International Journal of Signal Processing, Image Processing and Pattern Recognition, vol. 2, pp. 271-286, 2 2016.

[34] D. D. a. A. S. A. Shankar, "Minor blind feature based Steganalysis for calibrated JPEG images with cross validation and classification using SVM and SVM-PSO," Multimedia Tools and Applications , pp. 4073-4092, 2021.

[35] O. e. a. Yelamos, "Understanding Color," Photography in Clinical Medicine, vol. 2, no. 3, pp. 99-111, April 2020.

[36] J. Z. H. Q. K. T. W. Z. Z. G. L. &. Y. Y. Du, "RGB-IR cross input and sub-pixel upsampling network for infrared image super-resolution," Sensors, pp. 1-281, 2020.

[37] A. Villada, Shape Memory Structures and Electronics for Applications in Soft Robots and Biosensing Wearables, Colorado : University of Colorado at Boulder, 2020.

[38] T. J. a. M. T. B. Shah, A Review of Contemporary Image Compression Techniques and Standards, Examining Fractal Image Processing and Analysis, 2020, pp. 121-157.

[39] D. Q. Z. G. Q. Z. X. L. C. Y. &. W. F. Liu, "FPGA-based on-board cubic convolution interpolation for spaceborne georeferencing.," he International Archives of Photogrammetry, Remote Sensing and Spatial Information Sciences , vol. 15 , no. 7, pp. 349-356, June 2020.

[40] S. D. R. a. L. T. C. Mao, "Deep residual pooling network for texture recognition,"

Annals of R.S.C.B., ISSN:1583-6258, Vol. 25, Issue 6, 2021, Pages. 10697 - 10718
Received 25 April 2021; Accepted 08 May 2021.

Pattern Recognition, vol. 33, no. 2, pp. 213-220, 2021.

[41] M. A. a. K. G. Gungor, "Developing a compression procedure based on the wavelet denoising and JPEG2000 compression," Optik , vol. 18, no. 5, pp. 36 - 58, Sep 2020.